

Aeromagnetic Mapping of PreCambrian Geological Structures That Controlled the 1968 Meckering Earthquake (M_s 6.8), Western Australia

Mike Dentith (corresponding author)

School of Earth & Environment

The University of Western Australia

Nedlands

Western Australia 6009

Australia

Fax: +61 8 6488 1037

Email: mdentith@segs.uwa.edu.au

Dan Clark

Geoscience Australia

GPO Box 378

Canberra

Australian Capital Territory 2601

Australia

Fax: +61 6249 9986

Email: Dan.Clark@ga.gov.au

William Featherstone

Western Australian Centre for Geodesy

Curtin University of Technology

GPO Box U1987

Perth

Western Australia 6845

Australia

Fax: +61 8 9266 2703

Email: W.Featherstone@curtin.edu.au

Abstract

The 1968 Meckering earthquake (M_s 6.8) resulted in the formation of an extensive surface rupture complex comprising faults with a range of orientations and demonstrating reverse and dextral lateral offsets. The rupture extended for approximately 37 km and scarps reached up to 2.5 m high near to the centre of the complex. Modeling of the seismological characteristics of the source show reverse failure occurred on a north-south striking, east-dipping, surface, but how this is related to the local Precambrian bedrock geology is not clear.

Interpretation of new aeromagnetic data, together with subsequent ground-truthing, has allowed concealed bedrock lithology and structure to be mapped in previously unachievable detail. These data show that the surface faulting correlates closely with linear magnetic anomalies, interpreted as dykes/faults and lithological contacts. The apparent arcuate form of the fault complex is explained in terms of the reactivation of northeasterly (dykes and faults) and northwesterly (stratigraphic) trending features in a stress regime with an east-west oriented maximum principal stress. Space problems created where these two trends converge led to the creation/reactivation of a linking north-south trending thrust fault which accommodated the greatest displacements recorded for the 1968 event. This interpretation is consistent with previous research on the source parameters of Meckering event, which invoked one or more easterly dipping failure surfaces and reverse slip.

Keywords

Aeromagnetism, faulting, intra-plate seismicity, Meckering, Western Australia

Introduction

Most attempts to explain occurrences of intra-plate seismicity invoke a zone of weakened lithosphere created during previous tectonic events (Johnston and Kanter, 1990). This is usually referred to as the 'zone of weakness' model. Examples of zones of lithospheric weakness correlated with modern intraplate seismicity include palaeorifts and major suture structures (ancient plate or terrane boundaries). There has been little research on 'zones of weakness' at the scale of individual intra-plate seismic events, i.e. relating individual earthquakes to specific faults. This paper describes detailed mapping of bedrock geology, using aeromagnetic data, in the vicinity of the Meckering earthquake (M_s 6.8, ML 6.9) that occurred on the 14th October 1968 near the small town of Meckering in the southwest of Western Australia (Fig.1). This occurred within the Southwest Seismic Zone (SWSZ), a zone of intra-plate seismic activity in the southwest of Western Australia (Doyle, 1971; Dentith and Featherstone, 2003).

The Meckering earthquake was associated with extensive surface rupture; a 37 km long arcuate complex of mainly dextral and reverse faults was created (Everingham et al., 1969; Gordon and Lewis, 1980). In fact surface faulting may be quite common in the southwest of Western Australia where seismicity is unusually shallow (Leonard, 2008). Three historic events have produced surface faulting (McCue, 1990) and there may be many more palaeoscarps in the region (Clark, in press).

Geologically, the Meckering earthquake occurred within the Yilgarn Craton. The local bedrock comprises Achaean high-grade metamorphic rocks and Proterozoic dykes. The local terrain is subdued and outcrop is exceptionally poor. However, the nature of the bedrock is amenable to mapping using aeromagnetic data because of the large contrasts in magnetism in the local rocks. Low-level, high-resolution, aeromagnetic surveys are routinely used in mineral exploration in Western Australia and the expertise to acquire and process such data are therefore readily available. The resulting data allow the bedrock geology to be mapped with previously unattainable confidence and detail, and when combined with published seismological studies of the 1968 Meckering event, allow the influence of the local geology on the location and characteristics of this significant seismic event to be ascertained.

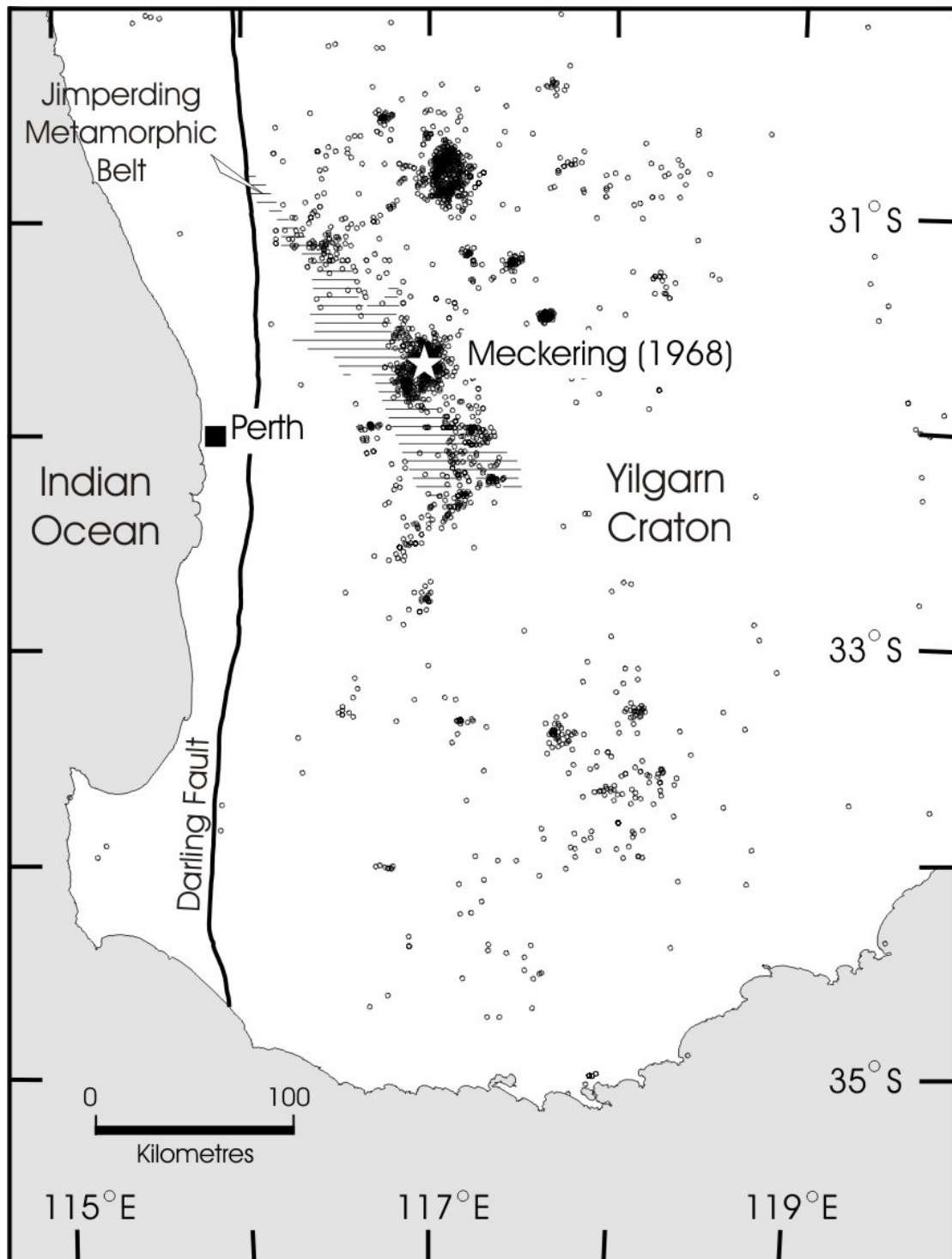


Figure 1. Map of the southwest of Western Australia showing the position of the 1968 Meckering event and other epicentres in the Southwest Seismic Zone (1960-1999, $ML > 2.0$).

Geology of the Meckering Area

The most detailed description of the geology of the Meckering area is that of Lewis (1969). Exposed bedrock consists of poorly exposed mafic (quartz dolerite) dykes that intrude various types of granitoid. It is not possible to determine the relationships between the different

granitoids, and often individual outcrops contain a range of lithotypes. Post-cratonisation mafic dykes, comprising a number of swarms with different orientations and ages, are common in the Yilgarn Craton (Hallberg, 1987). The dykes near Meckering have a variety of orientations. The dominant trend is northeast-southwest, with a much smaller number of dykes trending westnorthwest-eastsoutheast or northwest-southeast. Dykes with the former trend may contain numerous granitic xenoliths. The dykes vary in width from some tens of centimeters to around 30 m. They are notable for their high Koenigsberger ratios, i.e. their remanent magnetism is usually dominant.

Evidence for other rock types in the area is seen in the face of a currently disused aggregate quarry, located a few kilometres west of Meckering. Figure 2a shows the western face, where metre-scale xenoliths of amphibolite occur within a porphyritic granitoid. Figure 2b shows a second, much smaller, type of xenolith found in the quarry. These are calcsilicate rocks and are interpreted as metamorphosed carbonate sedimentary rocks. Similar rocks occur in the Jimperding Metamorphic Belt (Wilde, 1980), which is exposed a few tens of kilometers to the west and north of Meckering (Fig.1). The large xenoliths suggest the quarry lies close to the roof of the granitic intrusion. Exposures of the mafic dykes demonstrate their association with faults. Figure 2c shows a minor granitic intrusion offset, in a reverse sense, across a dyke.

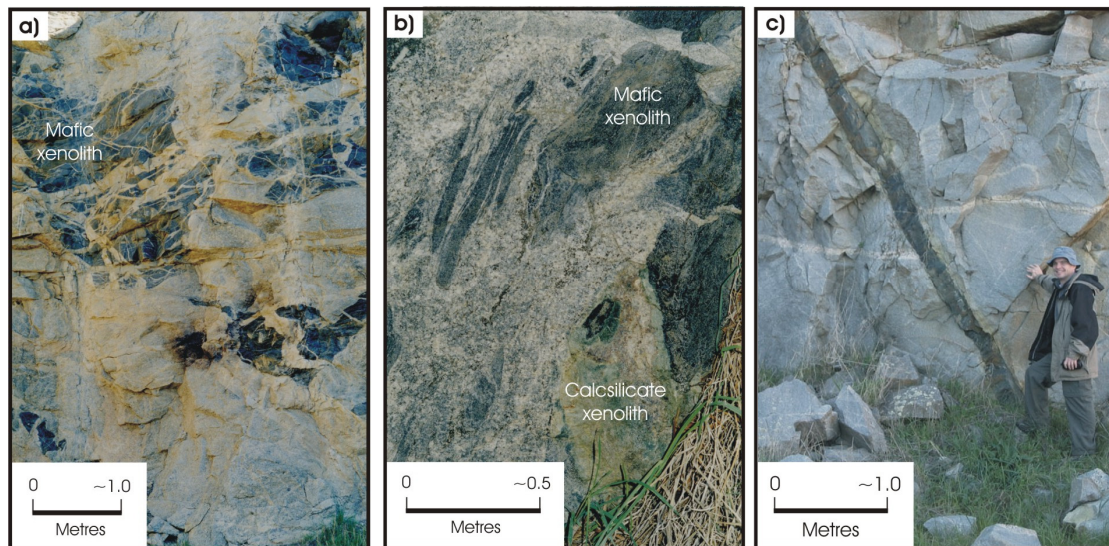


Figure 2. Rocks exposed in the Meckering quarry. a) Western face. The dark coloured areas are xenoliths composed of amphibolite and intruded by veins of aplite. The lighter coloured rock is porphyritic granite. b) Xenoliths of calcsilicate rocks in granite. c) Northeast-trending mafic dykes showing association with displaced late-stage granitic vein and southeasterly dip.

Superficial deposits in the study area consist of massive ferricrete, iron-rich pisolitic gravel and aeolian sand and alluvium. Lines of drainage along valley floors typically overlie buried inset valleys that can contain several tens of metres of Tertiary fluvial sedimentary fill (de Broeckert & Sandiford, 2005).-

The 1968 Meckering Earthquake

Evidence for the type of failure associated with the 1968 Meckering event comes from three sources; studies of the surface faulting, seismological studies, and modelling of surface deformation. Note that the epicentre of the 1968 event, shown in Figure 3a, was derived from data from a sparse regional seismic recording network and is probably only accurate to within 20 km.

Surface faulting

The characteristics of the surface faulting created by the Meckering earthquake are described in considerable detail by Gordon and Lewis (1980); their study includes detailed maps of the distribution of faults and associated structures and determination of displacement at the surface. Figure 3a shows the main faults and Figure 3b the observed changes in elevation and horizontal displacement vectors. Displacements were determined from offset linear features, such as fence lines, a water pipeline and a railway line.

Gordon and Lewis (1980) named a number of individual faults that comprise the surface fault complex (Fig.3a). The major structures are the Meckering, Burges, Splinter, and Robinson Faults, which accommodated most of the strain associated with the earthquake. These faults were distinguished from those such as the Chordal Fault, which were thought to be the result of strain accommodation in the hangingwall block subsequent to displacement along the main faults.

The dip of the Meckering Fault, measured at the surface, varies between 35° and 52° towards the inside of the arc, i.e. easterly. Referring to the displacement vectors in Figure 3b, the main movements on the Meckering Fault are compressional, with varying amounts of dextral strike-slip. The maximum displacement, both laterally and vertically, occurs on the approximately north-south trending central segment of the Meckering Fault. Here there is a westward heave of 2.44 m, a dextral lateral component of movement of 1.54 m, and a throw of 1.98 m. To the northwest of this location displacements are in the same, roughly westerly, direction. However, to the south the displacement directions are more southwesterly.

The Splinter Fault is a dextral thrust fault about 9 km in length, which comprises the northwestern part of the surface fault complex. Its average dip at the surface is 27° to the southeast. The Burges Fault Complex and its continuation to the west, the Robinson Fault,

comprise thrust and dextral reverse faults. The position of these faults is often indicated by the presence of en-echelon tension features in the cover. To the west, the Robinson Fault is terminated by a northwest-trending structure composed of thrust faults and en echelon tension fractures.

Gordon and Lewis (1980) describe the Sudholz Fault as having indications of minor normal and sinistral displacements. The much longer Chordal Fault is also described as being associated with small normal displacements, but in this case lateral movements were dextral, these being greater towards the southern end. Displacements reach a few tens of centimetres. The Chordal Fault, and possibly the Sudholz Fault too, appeared weeks to months after the main event and are thus considered to be the result of strains in the hangingwall of the fault complex caused by the main seismic event.

Gordon and Lewis (1980), in attempting to formulate a synthesis of the observed pattern of faulting, emphasized characteristics that they interpreted as indicative of arcuate and radial components. They proposed a model where the Meckering Fault is assumed to represent a quadrant of a complete circle and to have a lesser dip at depth than at the surface. A saucer-like “spherical cap” approximately 20 km in diameter was postulated, whose western/northwestern edge coincides with this fault. Trending northwest and passing beneath the centre of the cap, a vertical sinistral shear zone is proposed. Subsequent seismological studies suggest this model is unlikely, as discussed in the following section.

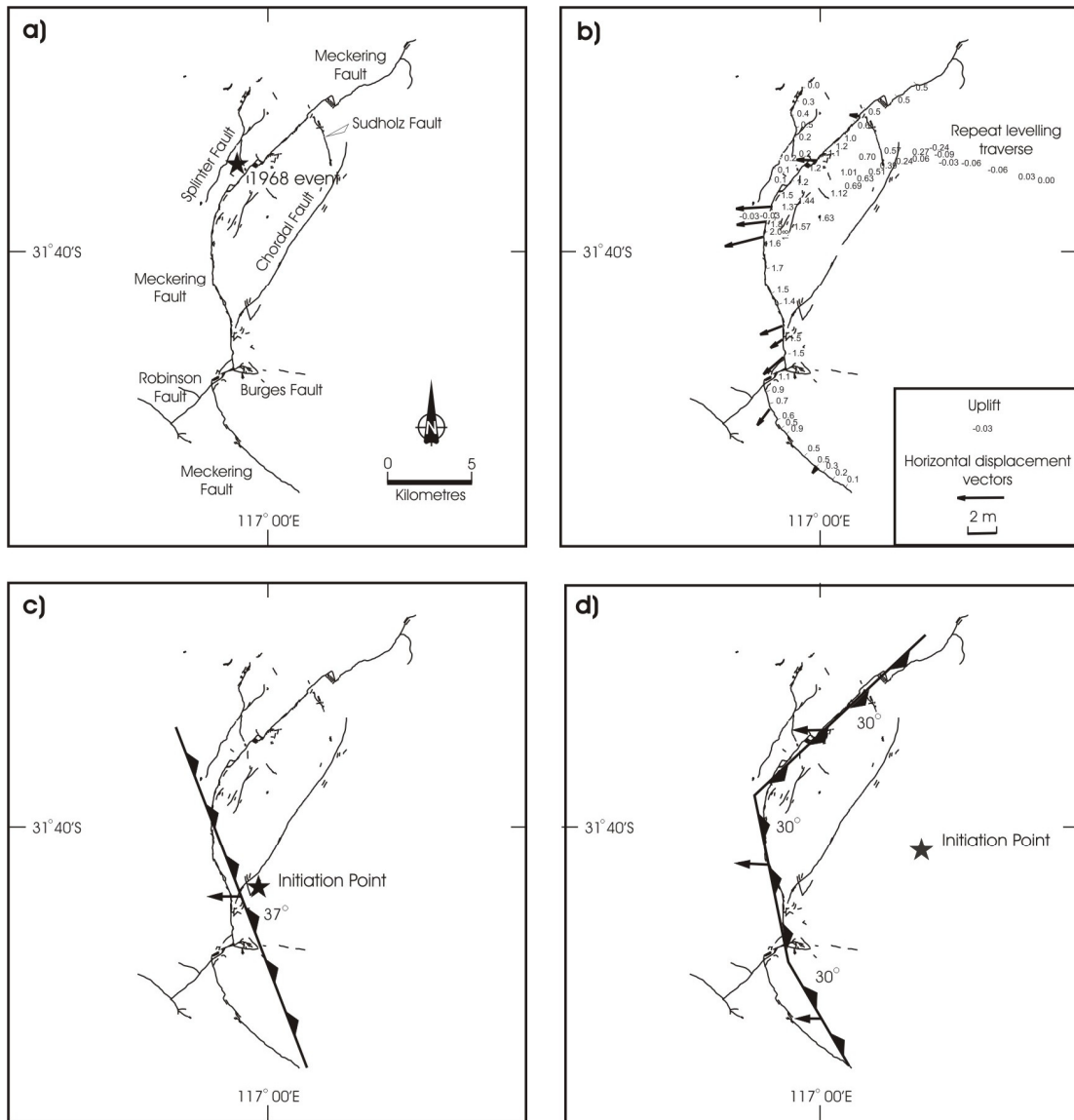


Figure 3. a) Map of surface faulting created by the 1968 Meckering event showing named faults. b) Measured uplift in metres (figures) and displacement vectors (arrows) associated with the surface faulting/earthquake. Note the maximum throw and heave occurs in the roughly north-south trending section of the fault scarp. Based on data in Gordon and Lewis (1980). c) Position of planar fault surface inferred by Vogfjord and Langston (1987) in relation to surface faulting, d) as for c) but with non-planar fault model.

Seismological studies

There are several published analyses of the mechanism of faulting associated with the 1968 Meckering event. In an early study, Fitch et al. (1973) studied long-period recordings of P-wave first motions and S-wave polarisations using data from WWSSN stations, supplemented by recordings from Australian arrays. Fitch et al. (1973) comment on the “complexity” of the Meckering event, stating the P-wave character is strongly suggestive of a multiple rupture and

postulate a foreshock 3.5 s prior to the main shock. This foreshock was thought to have a different mechanism to the main event. Fitch et al.'s preferred interpretation of the main Meckering event comprises a significant strike-slip component (Fig.4a). The preferred fault plane trends northwest-southeast (332°) and has a steep dip (68°) to the southwest, making the strike-slip sinistral. As noted by other workers (see below), this is at odds with the field observations of reverse-dextral movements on shallow dipping faults, but is consistent with the model of Gordon and Lewis (1980) who interpreted the surface faulting as caused by an underlying northwest-trending sinistral strike-slip feature (see above).

The most detailed study of the Meckering event is described by Vogfjord and Langston (1987) and Langston (1987). Vogfjord and Langston (1987) analysed long- and short-period WWSSN recordings of the Meckering event, and used a linearised inversion of long-period body-wave data to obtain a moment tensor and source-time function. Input to the inversion were 20 P and 5 SH data recorded at teleseismic ranges. A source depth of approximately 3 km was preferred, based on various error measures. The preferred focal mechanism is almost pure thrusting, with the fault plane trending almost north-south (Fig.4b). With this mechanism, synthetic and observed data from the main event were in good agreement, with mismatches at later times justified in terms of crustal reverberations. The predicted pressure axis is well constrained as sub-horizontal, and approximately east-west. Vogfjord and Langston (1987) also recognise complexities in the data, including the foreshock, and suggest "a finite source allowing failure on a nonplanar fault might have to be incorporated to explain the radiation pattern completely". These authors attempted to match both long- and short-period P-wave data in terms of a propagating dislocation source, with a given rupture velocity, on a finite fault. The best match was a radially downward propagating rupture, on a single planar fault, initiated at a depth of 2 km (Fig.3c), although it was noted that some observed waveforms were not well-matched. The resulting fault plane is semi-circular and extends to a depth of 5.7 km. An alternative "non-planar" model comprising three linked segments oriented to match the surface faulting (Fig.3d) and upward radially propagating rupture, initiating at 5.2 km depth, produced an equally good fit for the long-period data. However, the fit was considered poorer for the short period data, which would normally be better at constraining the details of the rupture geometry.

Langston (1987) analysed 11 foreshocks and 48 aftershocks from the Meckering earthquake to discover the depth distribution of faulting. The foreshock depths cluster at less than 2 km depth, and most of the aftershocks occur within 1 km of the surface.

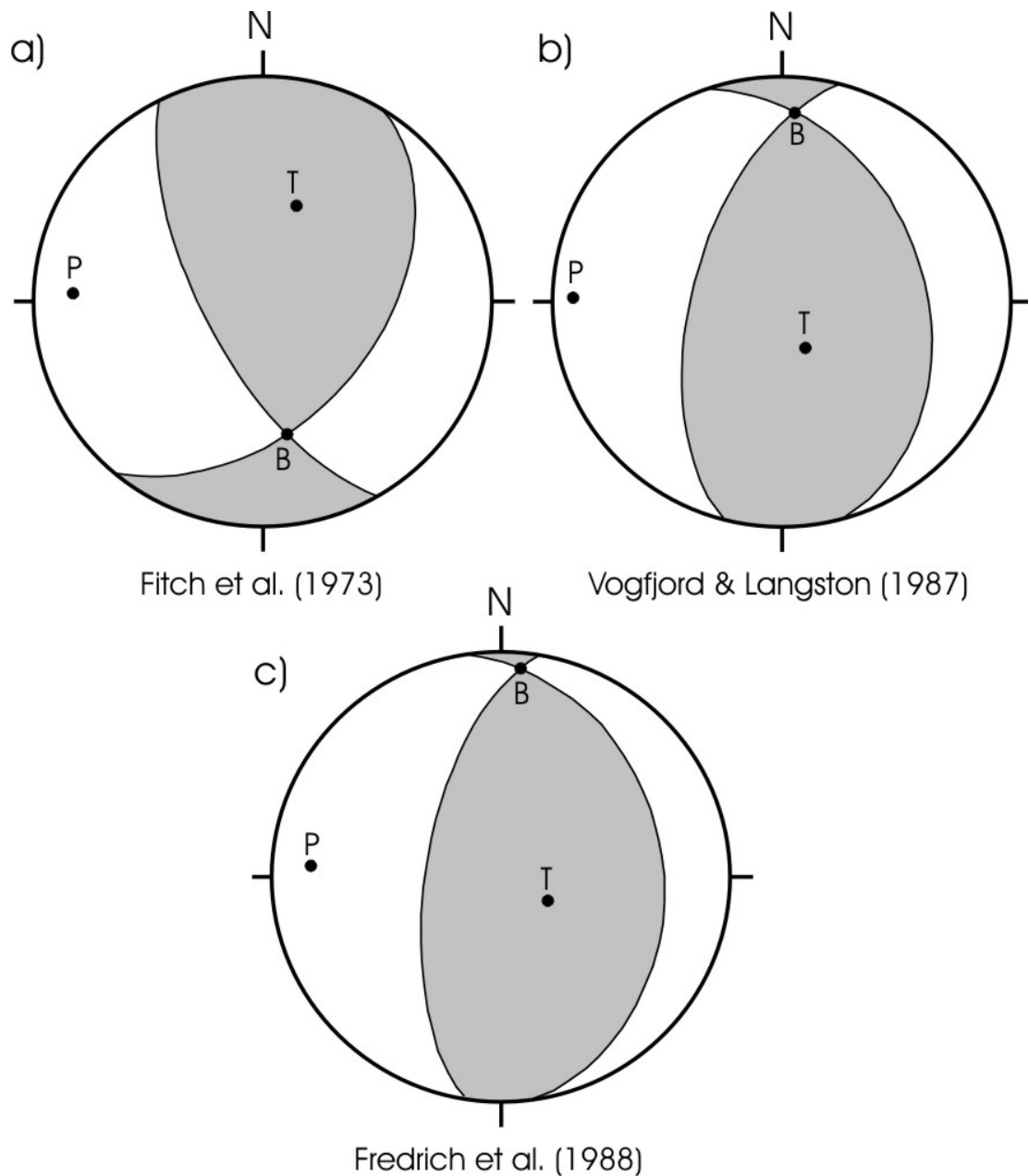


Figure 4. Published focal-mechanism solutions for events near Meckering.

Fredrich et al. (1988) modeled long-period teleseismic body waves from the Meckering event to create a fault-plane solution, source depth, seismic moment and source-time function, using a best-fitting double-couple point source. Modeling utilised P- and SH-waves at epicentral offsets of $30\text{-}90^\circ$ and $30\text{-}70^\circ$ respectively. Synthetic seismograms were constructed by combining direct P- and S-waves and reflected (pP and sP, or sS) phases. Inversion relied on minimising amplitude differences between observed and modeled data in a least-squares sense. The preferred model of the Meckering event was one of almost pure thrust faulting on a north-striking plane, with a centroid depth of 3 km (Fig.4c). Of the two alternatives, the faulting seen at the surface suggests the shallower east-dipping nodal plane is

the fault plane. This model is very similar to that of Vogfjord and Langston (1987). Uncertainties of the orientation of the nodal plane are of the order of 10° . Uncertainties in the centroid depth are greater, but Fredrich et al. (1988) argue for a depth of around 2.5-3.0 km. There is also evidence for a small precursor event 3.5 s prior to the main event, as noted by earlier workers. This was modeled with a mechanism identical to the main event, with modeling insensitive to the introduction of a strike-slip component as suggested by other workers.

Surface Deformation

The only attempt to quantitatively model the surface deformation associated with the Meckering earthquake is the work of Vogfjord and Langston (1987). Re-levelling data and measured displacements from the surface faulting (Fig.3b) were used to estimate a single east-west profile across the region of maximum uplift. This was modeled in terms of a rectangular fault, with constant displacement, embedded in an elastic half space. The observed deformation was modelled using a dip-slip fault with a dip of 37° to the east, a north-south strike, a dip-slip of 3.8 m and a (down-dip) width of 9.5 km. The observed and calculated data match reasonably well; however, the fact that the data are confined to a single traverse limits the significance of the results.

Comments on Faulting-Related Studies

From the various sources of data described above, there is general agreement that the Meckering event involved predominantly compressional deformation and that the hypocentre was at a depth of a few kilometres. The more sophisticated attempts to model the seismic recordings suggest reverse movement on a north-south striking, east-dipping, thrust fault.

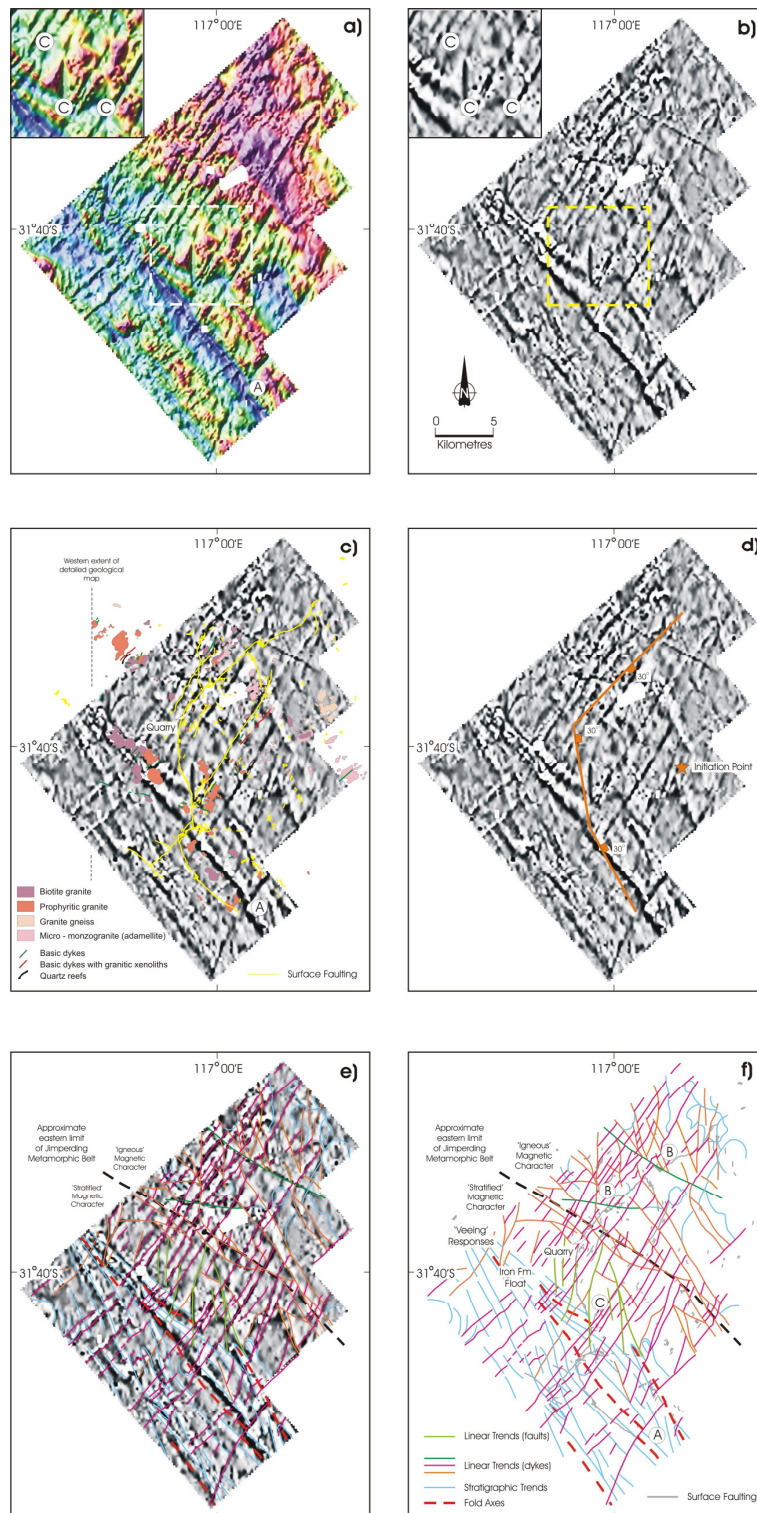


Figure 5. Total-field magnetic data from the Meckering area. a) TMI pseudocolour image, b) TMI grey-scale separation-filtered image. The insets are an enlargement of the areas within the dashed rectangle. c) TMI grey-scale separation-filtered image with outcrop geology and surface faulting overlain. d) same as b) but with fault planes inferred, based on of seismological studies, by Vogfjord and Langston (1987) overlain, e) and f) interpretation of aeromagnetic data. ‘A’ etc are features referred to in the text

Meckering Aeromagnetic Survey

The aeromagnetic survey of the Meckering area comprises a total of 3179 line kilometres flown with a fixed-wing aircraft at a line spacing of 200 m and a height of 30 m. The subdued topography meant a constant ground clearance was easily maintained, although regulations regarding flying in residential areas meant flying was prevented over the Meckering town site itself. Total magnetic intensity (TMI) was measured as well as GPS position and ground clearance. Lines were flown east-west, so as to be orthogonal, as far as is possible, to the major trends within the surface fault complex. Along-line sampling is at intervals of about 7 m. The survey specifications are typical of those used in large-scale surveys for area selection in mineral exploration in Western Australia, albeit at a lower than normal altitude. Experience has shown that the essential features of a geological setting such as at Meckering can be defined by surveys with such specifications.

Data Processing

There were no particular problems associated with acquisition, processing and imaging of the Meckering magnetic dataset. The main difficulty was associated with cultural features, specifically farm and residential buildings which give rise to localised high-amplitude magnetic responses. The cultural features were mostly successfully filtered out based on their short wavelength, and where this proved impossible the contaminated areas of the dataset were excised. Such areas, plus the town site, are responsible for the ‘holes’ in the images depicted in Figure 5.

Overall, the aeromagnetic survey was highly successful and the resulting data allow bedrock structure and lithology to be mapped with considerable confidence. The interpretation presented here is based primarily on the TMI and separation filtered versions of the data, which tests showed to be most useful (Fig.5).

Magnetic Susceptibility Data

To assist in the interpretation of the aeromagnetic data, magnetic susceptibility was measured randomly over outcrops at 39 sites in the Meckering area. Additional data were collected a few tens of kilometers to the west, where rocks of the Jimperding Metamorphic Belt are exposed. At each site 50 readings were made with a hand-held susceptibility meter (Exploranium model KT5). These data, organised where appropriate according to the lithotype assigned to the particular outcrop by Lewis (1969), are shown in Figure 6. The dyke dataset is small due to limited outcrop. The xenolith data come from a single locality, i.e. the Meckering quarry (Figs.2 and 5).

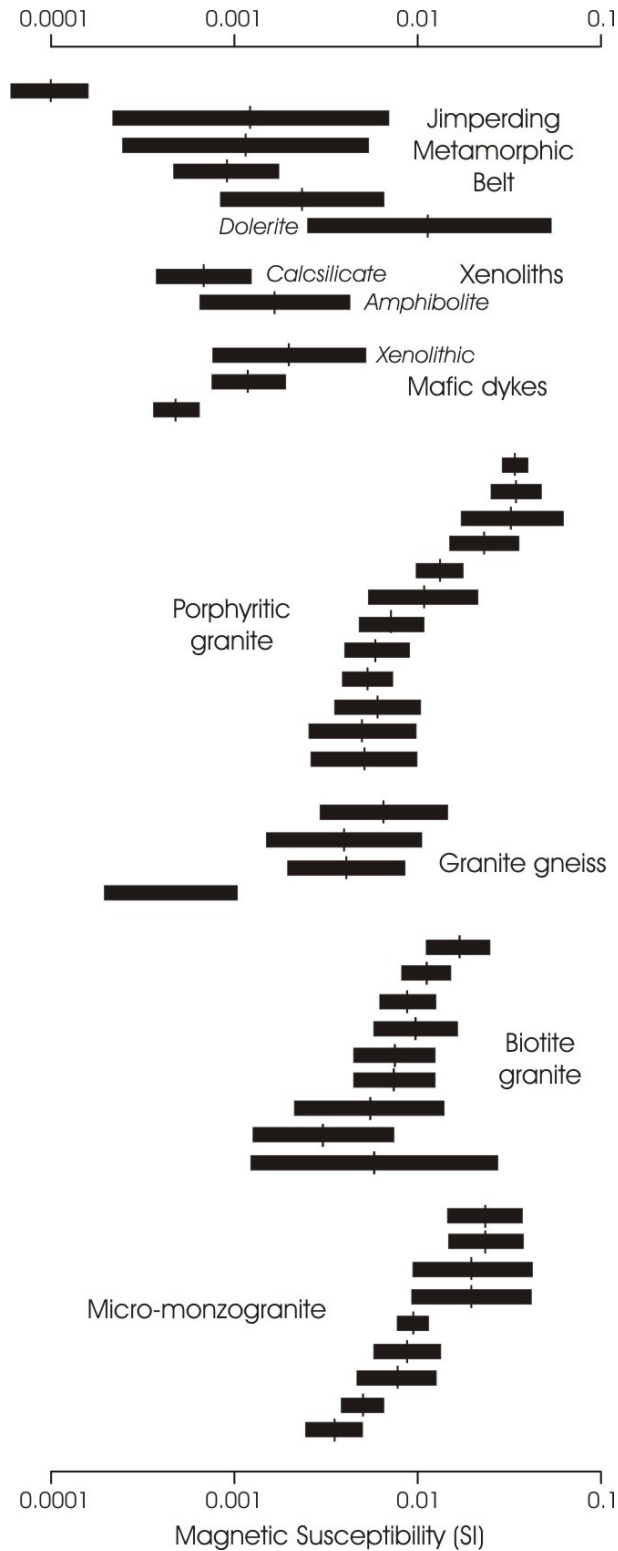


Figure 6. Magnetic susceptibility readings from outcrops in the Meckering area and nearby Jimperding Metamorphic Belt. Granitoid lithologies are assigned based on the mapping of Lewis (1969). The geometric mean and standard deviations of the data from each site are represented by the vertical line and horizontal bar, respectively. Each dataset comprises 50 measurements. The exception is the meta-sedimentary xenoliths, the limited outcrop allowing only 10 measurements to be made.

The susceptibility values in the area vary by approximately two orders of magnitude, which is sufficient to explain the observed variations in TMI. The most significant aspect of the data is the relative susceptibilities of the granitoids, xenoliths and rocks of the Jimperding Metamorphic Belt. The granitoids are clearly the most magnetic rocks in the survey area. The variations between what are mapped as the same lithotypes are indicative of the mix of rock types at each outcrop and variations in the amount of mafic component. For example, the outcrop of gneissic granite with abnormally low susceptibilities is particularly felsic in composition. The rocks of the Jimperding Metamorphic Belt are migmatitic gneisses, plus one exposure of doleritic material. The susceptibilities are significantly less than those of the granitoids exposed near Meckering, with the exception of the doleritic exposure. The meta-sedimentary xenoliths from the Meckering Quarry have comparable susceptibilities to the migmatitic gneisses. The mafic xenoliths seen in the quarry vary from values similar to the dykes to values comparable to the rocks of the Jimperding Metamorphic Belt.

The mafic dykes have a susceptibility range that lies between those of the gneisses and the granitoids. The Proterozoic dykes in the Yilgarn Craton often have high Königsberger ratios; with several dyke sets known to have reversed remanent magnetism resulting in negative anomalies. This means the dykes are likely to cause significant anomalies in the magnetic data despite the measured susceptibilities.

Interpretation of Aeromagnetic Data

Images of TMI from the Meckering survey are shown in Figure 5a and 5b. In Figure 5c the same data are shown with the local geology overlain and in Figure 5d the non-planar failure surfaces inferred by Vogfjord and Langston (1987) is overlain. An interpretation of the aeromagnetic data is shown in Figures 5e and f.

TMI varies by several hundred nanoTesla and is generally greater in the northeastern part of the survey area than in the southwest, e.g. Figure 5a. The area to the northeast resembles the responses expected in a terrain composed of granitic igneous and metamorphic rocks. However, to the southwest the linear magnetic variations are consistent with responses from a succession with laterally persistent, lithological layering. The linear features in the southwestern half of the data define a 'V-shaped' feature, consistent with an anomaly pattern expected from a plunging fold; compare Figures 5e and 5f. The rocks comprising the inferred fold structure are most likely the eastward continuation of the Jimperding Metamorphic Belt (Fig.1), which contains folds with a similar orientation (Wilde, 1980). This interpretation is supported by the observation that calcsilicate rocks similar to those seen in the Meckering quarry also occur in the Jimperding Metamorphic Belt. The fold axis trends towards the northwest, but in the absence of facing information the type of folding cannot be determined.

The symmetrical response suggests a near upright structure. It may be significant that the linear anomalies coincide with a place where iron formation-float occurs as numerous fragments in the soils (Gordon and Lewis, 1980; Fig. 5f). Iron formation is known from the Jimperding Metamorphic Belt and linear magnetic anomalies are consistent with a gneissic bedrock; consistent with the continuation of the Jimperding Metamorphic Belt in to the Meckering area, as shown in Figure 1.

Also of interest is the fact that the pattern of outcropping granitoids does not closely correspond with the pattern of magnetic variations. One explanation is that the outcrop in the southwestern part of the survey area is not representative of the bedrock. That is, weathering-resistant granitoids are the only exposed rock type despite being a comparatively minor constituent of the bedrock. In places, localised positive magnetic anomalies crosscut the linear grain. This is probably due to the near-surface granitoids. As noted previously, the large xenoliths in the Meckering quarry (Fig.2a) suggest this location is near the roof of the intrusion. The quarry lies close to the transition from the 'granitoid' responses in the northeast and the 'layered' response in the southwest. Thus, it is consistent with the interpretation of the bedrock to the southwest being composed of a succession of rock types such as are preserved as xenoliths, i.e. meta-sedimentary and meta-igneous rocks.

Extending across the entire magnetic survey area are prominent, slightly curved, linear anomalies that mostly trend roughly northeast-southwest. In the north of the survey area there are a few similar anomalies that trend northwest-southeast, and east-west. Some of these anomalies coincide with exposed mafic dykes, which are almost certainly their source. In some cases, 'stratigraphic' anomalies are clearly displaced on either side of the dyke anomalies (notably the locations labeled 'A' in Figure 5), indicating the dykes either intruded along faults, or have been sites of subsequent faulting. This is consistent with observations in the Meckering Quarry (Fig.2c).

The significance of the aeromagnetic data becomes apparent when the 1968 surface faulting is overlain (Figs 5c). Almost every occurrence of faulting is associated with linear features in the magnetic data. This is consistent with geological evidence that the surface faulting at Meckering involved reactivation of pre-existing structures; specifically, iron-stained fault breccia within the exposed fault plane, an association of faulting with quartz float and a distinctive red-coloured soil and differences in the soil profile in pits dug on either side of the fault (Gordon and Lewis, 1980).

In southern part of the survey area, the Meckering Fault parallels the linear anomalies interpreted as representing lithological layering in the core of the plunging fold. The implication is that lithological contacts in the basement have controlled the position of surface faulting. The Burges/Robinson, Chordal, Meckering, Splinter and Sudholz Faults all coincide with linear magnetic anomalies. The area where there are most northeast-trending faults

coincides with the greatest density of magnetic linears of this trend. Of course there are many linear features in the dataset, but even so the correspondence between the faults and the anomalies is striking; even the minor apparent dextral offsets near the northern end of the Meckering Fault coincide with cross-cutting anomalies, in this case the northwest-southeast and east-west trending linears (labeled 'B' in Figure 5). Where the Meckering Fault trends north-south, and where its displacement is greatest, there is also a prominent magnetic linear, which is one of several in the vicinity (labeled 'C' in Figure 5f). However, this appears different to the dyke anomalies; it being narrower and with a different trend.

Discussion

Since there is general agreement that the Meckering rupture initiated at a depth of a few kilometres, it is reasonable to extrapolate the geology inferred from the magnetic data to hypocentre depths. Based on the inferred fold, the dominant lithologic trend in the area is interpreted to be northwesterly. The dips of the lithological contacts are unknown, but based on the geology of the region to the northwest are likely to average about 45° (Wilde, 1980). The other important trend is nearly orthogonal and is associated with mafic dykes, which are also the sites of faulting. The dyke with this trend in the Meckering Quarry dips southeastwards at about 60° (Fig.2c). Recall that the most reliable focal mechanism studies suggest reverse faulting occurred on a north-south trending structure in regional stress field with an east-west oriented maximum principal stress.

A schematic illustration of the interpreted geological controls on the Meckering earthquake and associated surface faulting is shown in Figure 7. The two major geological trends are suitably oriented for failure in an east-west oriented compressional stress field. There will be reverse-dextral movements on the northeast-southwest trend (as is observed, Figure 3b). Any lateral movements associated with the northwest-southeast trend would be reverse-sinistral, but the lesser dip might encourage mainly reverse movements. Referring to Figure 3b, there is no evidence of the expected sinistral displacements, and instead the displacement vector is almost perpendicular to the fault trend. However, it is well known that existing faults locally rotate stress fields, e.g. Faulkner et al. (2006), and the combination of the fold hinge-parallel, and dyke-related, faults in this area may be complicating the situation.

The lateral movements on intersecting surface trends will create a space problem where the particular surfaces converge. This may be the reason why the Meckering Fault trends north-south at its most westerly extent. This part of the fault serves both to resolve the space problem and link the two zones of deformation on pre-existing structures and hence is probably the major failure surface. It is no coincidence that this part of the fault complex is, 1), where the maximum displacements occur (Fig.3), and 2) in the same orientation as the failure surface inferred from modelling of the seismic waveforms and surface deformation

(Fig.5) and has a different magnetic appearance. This interpretation is essentially identical the “non-planar” model of Vogfjord and Langston (1987), although derived from a completely independent dataset. Overlying the surface projection of the failure surface derived by these authors shows a correspondence of linears in the magnetic data, in particular the north-south trending linear anomaly interpreted as parallel to the main failure surface. The main failure surface is clearly evident in the aeromagnetic data (Fig.5a and b). As described earlier, Vogfjord and Langston (1987) preferred the single planar fault model. However, they acknowledge that the match to the observations was imperfect for both the models they describe and the aeromagnetic data provide significant support the non-planar model.

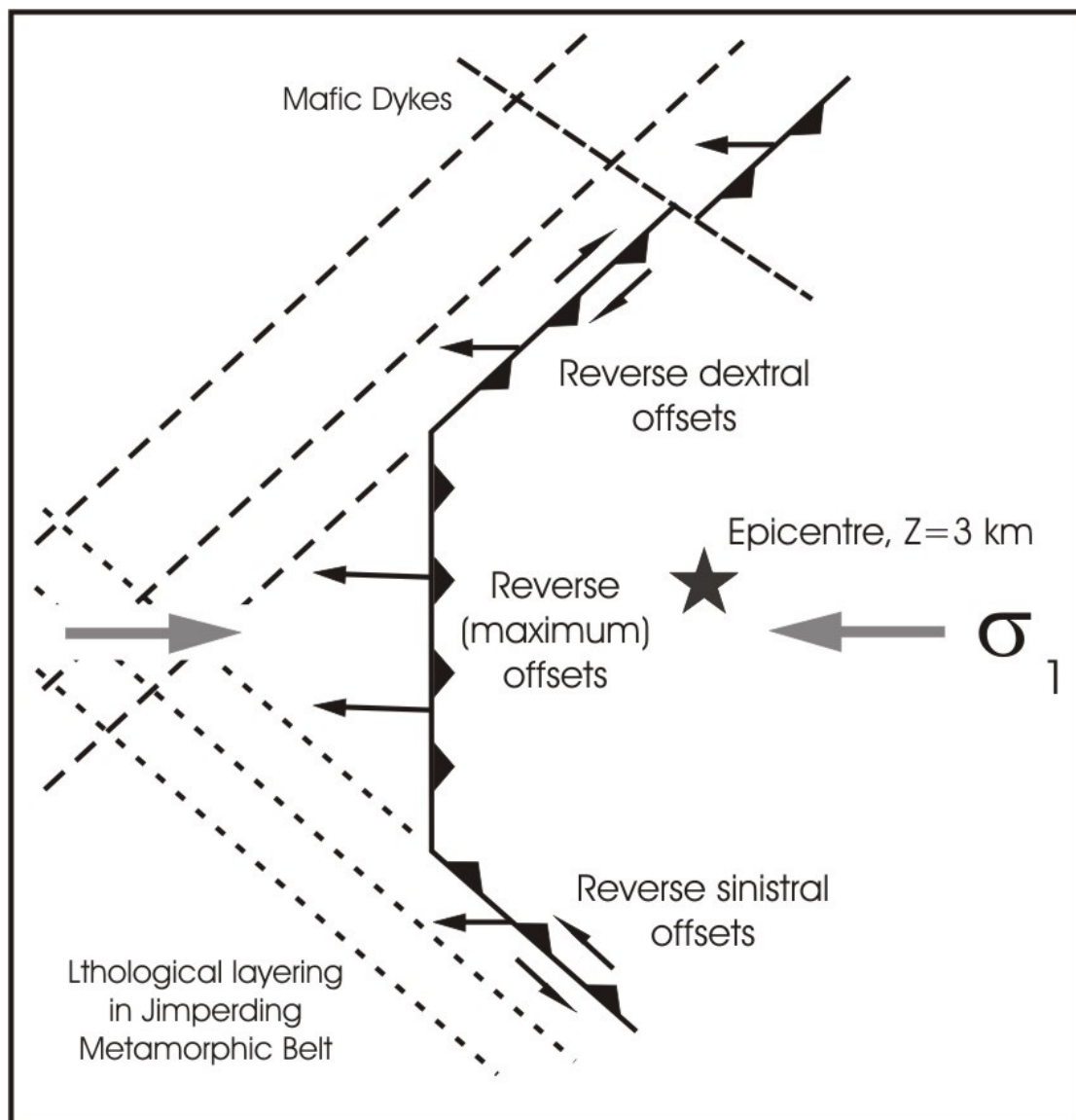


Figure 7. Schematic illustration of geological controls on the Meckering earthquake and associated surface faulting.

Summary

The Meckering earthquake of October 1968 created an extensive complex of surface faults. However, sparse outcrop prevented the relationship between surface faulting and bedrock geology from being fully understood. New aeromagnetic data have defined anomalies of structural and lithological origin that allow bedrock geology to be mapped with considerably more confidence. Contrary to one previously postulated faulting mechanism, which invoked arcuate and radial structures, the pattern of surface faulting is shown to be controlled by intersecting northwest-southeast and northeast-southwest trending structures in the basement. Deformation in response to the prevailing east-west compressional stress field caused movements on these structures. The space problem created where the two trends converge caused almost pure compressional failure on a linking north-south trending surface. The net result is an apparent arcuate form to the surface faulting. A similar interpretation of the geometry of the failure surfaces, based on of seismological data, was reached by Vogfjord and Langston (1987).

Acknowledgements

Landowners, too frequent to name, are thanked for co-operation during data acquisition. Ray Gordon is thanked for discussions on the Meckering faulting. Charter Mathison is thanked for assistance identifying the local lithotypes. UTS Geophysics is thanked for flying the Meckering survey for a very competitive price. The images of the aeromagnetic data were created by Cowan Geodata Services. Geoscience Australia is acknowledged for indirect funding assistance. Dan Clark publishes with the permission of the Chief Executive Officer of Geoscience Australia. This is TIGeR publication number XXX.

References

- Clark D., in press. Identification of Quaternary scarps in southwest and central west Western Australia using DEM-based hill shading: application to seismic hazard assessment and neotectonics. *Special Publication of the International Journal of Remote Sensing*.
- De Broeckert, P. and Sandiford, M. 2005. Buried inset-valleys in the eastern Yilgarn Craton, Western Australia: Geomorphology, age, and allogenic control. *Journal of Geology*, 113, 471-493.
- Dentith, M.C. and Featherstone, W.E., 2003. Controls on intra-plate seismicity in southwestern Australia. *Tectonophysics*, 376, 167-184.
- Doyle, H.A., 1971. Seismicity and structure in Australia. *New Zealand Royal Society Bulletin*, 9, 149-152.

- Everingham, I.B., Gregson, P.J. and Doyle, H.A., 1969. Thrust fault scarp in the Western Australian shield. *Nature*, 223, 701-703.
- Faulkner, D. R., Mitchell, T. M., Healy, D. and HEAP M. J., 2006. Slip on 'weak' faults by the rotation of regional stress in the fracture damage zone. *Nature*, 444, 922-925.
- Fitch, T.J., Worthington, M.H. and Everingham, I.B., 1973. Mechanisms of Australian earthquakes and contemporary stress in the Indian Ocean plate. *Earth and Planetary Science Letters*, 18, 345-356.
- Fredrich, J.T., McCaffrey, R. and Denham, D., 1988. Source parameters of seven large Australian earthquakes determined by body waveform inversion. *Geophysical Journal of the Royal Astronomical Society*, 95, 1-13.
- Gordon, F.R. and Lewis, J.D., 1980. The Meckering and Calingiri earthquakes October 1968 and March 1970. *Geological Survey of Western Australia, Bulletin 126*.
- Gordon, F.R., and Wellman, H.W., 1971. A mechanism for the Meckering earthquake. *Royal Society of New Zealand Bulletin*, 9, 95-96.
- Hallberg, J.A., 1987. Postcatonization mafic and ultramafic dykes of the Yilgarn Block. *Australian Journal of Earth Sciences*, 34, 135-149.
- Johnston, A. C., and L. R. Kanter, 1990. Earthquakes in stable continental crust, *Scientific American*, 262, 68-75.
- Langston, C.A., 1987. Depth of faulting during the 1968 Meckering, Australia, earthquake sequence determined from waveform analysis of local seismograms. *Journal of Geophysical Research*, 92, 11561-11574.
- Leonard M., 2008. One hundred years of earthquake recording in Australia. *Bulletin of the Seismological Society of America*, 98, 1458-1470.
- Lewis, J.D., 1969. The Geology of the Country Around Meckering. *Geological Survey of Western Australia, Record 1969/18*, 14 pp.
- McCue, K., 1990. Australia's large earthquakes and Recent fault scarps. *Journal of Structural Geology*, 12, 761-766.
- Vogfjörd, K.S. and Langston, C.A., 1987. The Meckering earthquake of 14th October 1968: A possible downward propagating rupture. *Bulletin of the Seismological Society of America*, 77, 1558-1578.
- Wilde, S.A., 1980. The Jimperding Metamorphic Belt in the Toodyay area and the Balingup Metamorphic Belt and associated granitic rocks in the southwestern Yilgarn Craton. *Excursion Guide, 2nd International Archaean Symposium, Geological Society of Western Australia*, 40 pp.